ELSEVIER

Journal of Nuclear Materials 312 (2003) 174–180

journal of nuclear materials

www.elsevier.com/locate/jnucmat

Analysis of CREVONA sodium loop material

Vaidehi Ganesan [a,*], V. Ganesan [b], H.U. Borgstedt [c]

[a] Division for PIE and NDT, Indira Gandhi Centre for Atomic Research, Kalpakkam 603 102, India
[b] Materials Chemistry Division, Indira Gandhi Centre for Atomic Research, Kalpakkam 603 102, India
[c] Forschungszentrum Karlsruhe, Institut für Materialforschung, D-76021 Karlsruhe, Germany

Received 24 July 2002; accepted 13 November 2002

Abstract

Stainless steel specimens equivalent to AISI type 304 taken from the CREVONA sodium loop (Forschungszentrum Karlsruhe, Germany), which was operated for more than 80 000 h, were analysed for microstructures and changes in chemical composition of depleted layers using SEM/EDAX. SEM micrographs were obtained in the cross-section of the specimens to reveal the thickness of the corroded layer. EDX analysis confirms depletion of Ni and Cr in the corroded layer. The leaching rates of chromium and nickel are obtained from the depleted layer width. These results are compared with the degraded layer and corrosion resistant node formation in sodium-exposed AISI type 316 SS specimens. The corroded layer widths of the specimens taken from the CREVONA loop determined using known models for life prediction like those proposed by Thorley and Tyzack are found to be much less than the actual layer widths observed experimentally after sodium exposure. The materials were exposed to flowing sodium for about 10 years.

1. Introduction

Austenitic stainless steels of different grades are used as structural materials in primary circuits of fast reactors owing to their good compatibility with pure sodium at high temperature, while 9Cr–1Mo steel is the choice in steam generators. Chemical interactions of hot sodium leading to solid state reactions with the structural materials make it important to arrive at the proper choice of materials for the construction of liquid metal cooled fast reactor circuits [1,2]. The choice of liquid sodium as heat transfer medium stems from the merits of its physical properties such as high boiling point, low vapour pressure, high thermal conductivity and good heat transfer properties in addition to favourable chemical and nuclear properties. Owing to this choice, the knowledge on corrosion of materials in sodium environment is of great importance. The chemical compatibility of sodium with structural materials is generally good when sodium is in its pure state. However, the presence of impurities such as oxygen and carbon combined with a suitable velocity and thermal gradients in a sodium system leads to more serious corrosion. The interaction and compatibility of sodium with AISI type 316 stainless steels have been extensively studied [3–12]. Though localized electrochemical corrosion is absent in sodium systems, liquid sodium can slightly dissolve some of the constituents of stainless steel at high temperatures, which can be transported and deposited in different regions [2]. This mass transfer is influenced by impurities such as oxygen because of the formation of ternary oxides of sodium, primarily sodium chromite, $NaCrO_2$. Being an interstitial element, carbon in sodium can easily diffuse in or out of stainless steel depending on its thermodynamic activity in sodium resulting in carburization or decarburization, which will influence the mechanical properties. The different processes involved in the corrosion by liquid sodium are

* Corresponding author. Tel.: +91-4114 480208; fax: +91-4114 480356.
E-mail address: vaidehi@igcar.ernet.in (V. Ganesan).

0022-3115/03/$ - see front matter
doi:10.1016/S0022-3115(02)01593-3

(1) loss of material by leaching and consequent reduction in wall thickness,
(2) preferential leaching of elements and generation of modified layer of inferior properties,
(3) formation of carburized/decarburized austenite layer and
(4) precipitation of carbides in the matrix.

In our earlier work [13], we have analysed the corrosion results obtained under static conditions. The observed corrosion data such as weight loss, depleted layer formation, changes in microstructures, etc. of annealed specimens vis-à-vis cold worked specimens under dynamic conditions were discussed in detail [13]. Two predominant corrosion processes applicable to austenitic stainless steels in liquid sodium are the selective leaching and the steady state corrosion. The former is pronounced with low oxygen levels in sodium and leads to ferritisation in the initial stages. Once the ferrite layer is formed, its growth is controlled by diffusion parameters. The weight loss data due to steady state corrosion can be correlated to volume diffusion coefficients. Simple boundary conditions can be used to explain the corrosion behavior in austenitic stainless steel-sodium systems.

In this paper, we will discuss the results and analysis of CREVONA sodium loop material (SS 304). This sodium loop was designed for creep-rupture tests of austenitic steels in the temperature range 823–873 K. Samples of the material were taken from the test sections of the circuit in regions of maximum temperature. Such samples offer the chance to analyse corrosion effects after long periods of operation time that are in the order of magnitude of those of reactor components.

2. Experimental parameters

CREVONA was one of the two sodium loops for material behavior testing in flowing sodium in Forschungszentrum Karlsruhe, Germany [14]. It was operated for creep-rupture tests of long duration, the integrated operation time exceeding 80 000 h at nominal conditions. The main loop was of figure-of-eight configuration with an electromagnetic pump of 5 $m^3\,h^{-1}$ at 4.5 bar capacity, a sodium-to-air cooler in the cold part, a recuperative heat exchanger and a 72 kW heater to supply the test sections with sodium of desired temperature and flow velocity. The high-temperature circuit of the system contained four parallel test sections equipped with loading and strain measurement devices for creep-rupture tests. The characteristics and typical sodium purity in the CREVONA loop are shown in Tables 1 and 2.

When the sodium loop was dismantled, after nearly 10 years of operation, specimens of AISI 304 SS from four different positions were obtained, and their surfaces and cross-sections were analysed. The following specimens namely,

Table 1
Characteristics and parameters of sodium loop-CREVONA [14]

Parameters	Quantity
Sodium volume (l)	500
Capacity of main heater (kW)	72
Number of test sections	4 + 1
Maximum temperature of test sections (K)	973
Flow velocity in test sections ($m\,s^{-1}$)	3
Cold leg temperature (K)	673
Purification system	Cold trap
Purity measurement	
Carbon	Foil equilibration at 973 K
Oxygen	Emf cell, chemical analysis
Dissolved metals	Sampling device

Table 2
Sodium purity in CREVONA [14]

Impurities	Concentration (ppm)
O[a]	≈1–2
C[b]	0.1
N[b]	9×10^{-4}
Fe	3.7–2.2
Cr	0.8–0.2
Mn	0.2
Ni	0.2
Sn	0.9
Bi	0.75
Pb	0.35
Zn	0.20

[a] Cold trap temperature of 398 K.
[b] Foil equilibration method.

(1) the reference material SS 304 as-received (the material of CREVONA tubing),
(2) sodium tube to test section-2 (>80 000 h at 823 K, $v_{Na} = 1.5\ m\,s^{-1}$,
(3) sodium tube to test section-4 (60 000 h at 823 K + 20 000 h at 873 K, $v_{Na} = 1.5\ m\,s^{-1}$),
(4) sodium tube to foil equilibration chamber (10 000 h at 973 K, low flow velocity)

were cut for analysing the corrosion layers. The positions of the test sections in the CREVONA loop are shown in the flow sheet Fig. 1.

3. Experimental results

Generally it is very difficult to obtain specimens exposed to sodium for extremely long durations (of the

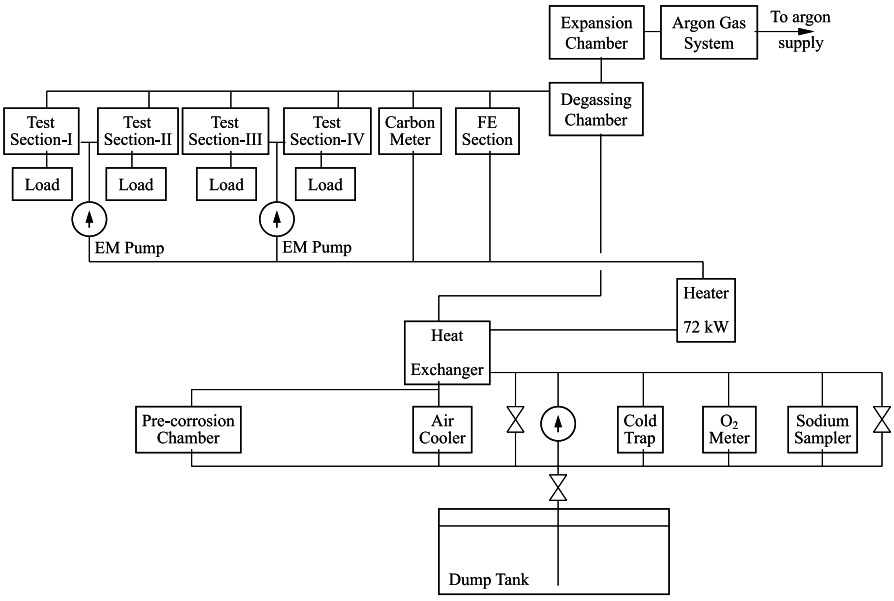

Fig. 1. General flow sheet of CREVONA loop.

order of 100 000 h and above). We have taken specimens exposed to high-temperature sodium for long durations from the CREVONA sodium loop [14] after dismantling. The corrosion behavior of these SS 304 specimens exposed to sodium is studied in this paper. The corroded layer thickness values are compared with those calculated using the model of Thorley and Tyzack [8]. In this study, depleted layer widths due to sodium corrosion in SS 304 have been obtained in an alloy without molybdenum. It will be a useful exercise to compare the depleted layer widths due to sodium exposure in SS 316, alloy D9 and SS 304 with the calculated values based on theoretical empirical models.

4. Analysis

AISI type 304 SS specimens from the CREVONA sodium loop were analysed for microstructures, and the microchemical analysis of depleted layers was performed using SEM/EDX. The above mentioned specimens were studied by means of metallographic and analytical methods. SEM micrographs were obtained in the cross-section of the specimens to reveal the thickness of the corroded layer. EDX analysis confirms depletion of Ni and Cr in the corroded layer.

The second specimen (Fig. 2) shows a non-uniformly degraded layer the thickness of which varies from 12 to

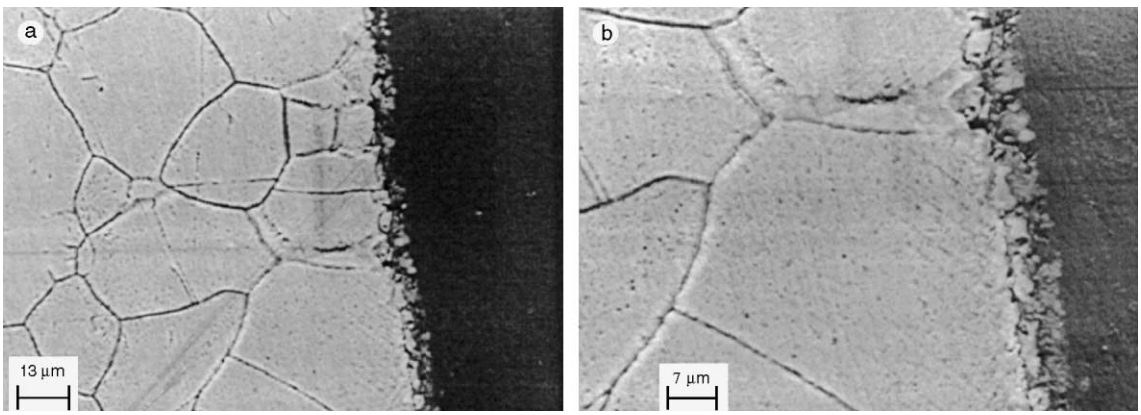

Fig. 2. Cross-section of tube to test section-2, exposed to Na for 80 000 h at 823 K showing Cr and Ni depleted layer and coarsened grain boundaries.

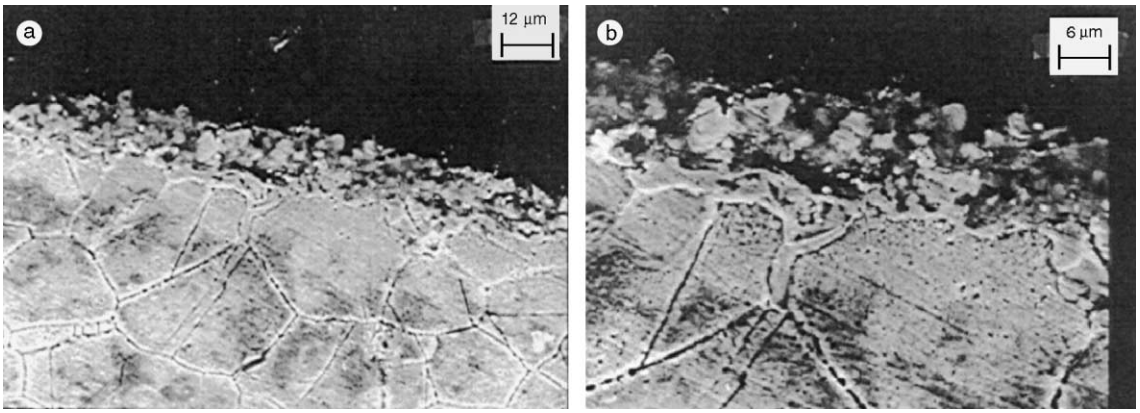

Fig. 3. Cross-section, tube to test section-4, exposed to Na for 80 000 h at 823 K and further 20 000 h at 873 K showing Cr and Ni depleted layer, coarsened grain boundaries, microcavities and decohesion in the ferrite layer.

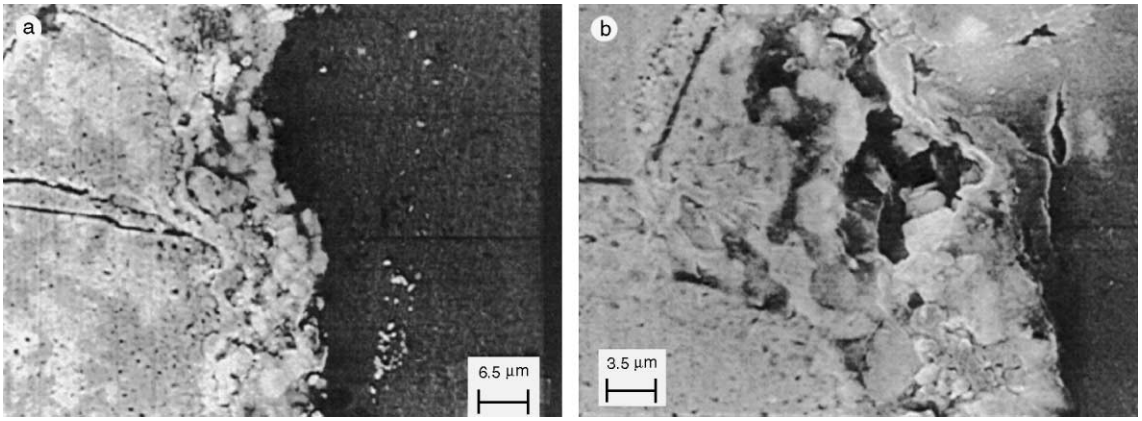

Fig. 4. Cross-section, tube to test Section-4, exposed to Na for 80 000 h at 823 K and further 20 000 h at 873 K showing Cr and Ni depleted layer and microcavities formation.

15 μm in some regions. The third specimen (Fig. 3) shows a non-uniform layer thickness of 18–20 μm, and a number of microcavities (Fig. 4) are also observed in the degraded layer. The fourth specimen showed a non-uniformly depleted layer of 10–12 μm (Fig. 5). Carbides were also observed only in this specimen (973 K, 10 000 h). Decohesion in the depleted layer occurred in some cases.

The leaching rates of chromium and nickel are obtained from the depleted layer width. These results are compared with the degraded layer and corrosion resistant node formation in sodium exposed AISI type 316 SS specimens [13]. The AISI type 316 SS specimens exposed to static and dynamic sodium reveal precipitates depleted in Ni and Cr, and corrosion resistant node formation. The depleted layer widths of SS 304 exposed to sodium are compared with results available in the literature. The microcavities observed in SS 304 specimens of the CREVONA sodium loop material after

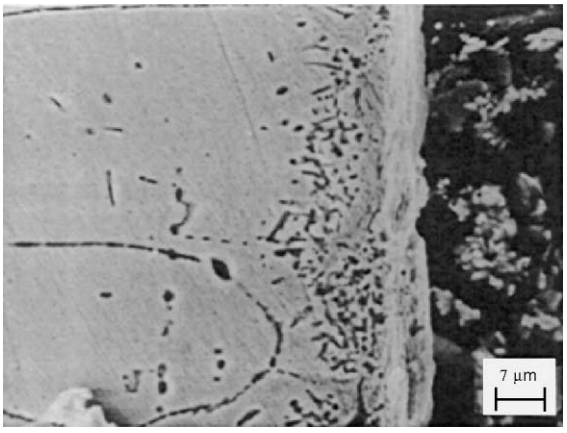

Fig. 5. Cross-section, tube to foil equilibration chamber, exposed to Na for 10 000 h at 973 K showing a depleted layer along with carbide formation and decohesion in the ferrite layer.

prolonged exposure to sodium further confirms the fact that alloys without molybdenum develop porosities in the surface regions due to sodium exposure. The corroded layer widths determined using known models for life prediction like those proposed by Thorley and Tyzack [8] for the above specimens are found to be much less than the actual layer width observed experimentally due to sodium exposure as shown in Table 3. The model of Thorley and Tyzack is stated to be general for all types of stainless steels. However, for SS 304 (CREVONA loop material) the calculated layer width and actual layer width are not comparable. There are two arguments:

1. alloys without molybdenum can corrode at a faster rate and
2. the model may not be suitable for high-temperature long duration of exposure to sodium.

If the oxygen content in sodium is not controlled there is the possibility of a higher depleted layer width due to increase in oxygen content. This is due to the tremendous increase in weight loss and depletion layer width with oxygen content in sodium (Table 4). But in this study, the oxygen content in the loop was continuously monitored by means of electrochemical oxygen meters and the oxygen concentration in the loop was maintained at 1–2 ppm. The chemical composition of major elements in SS 304 before exposure to sodium (in wt%) calculated from intensity of EDX peaks (approximately) is Cr = 18.3%, Ni = 9.7% and Fe = 68%.

The approximate chemical composition of the surface region of SS 304 specimens namely the Na-tube to test section-4 (60 000 h at 823 K + 20 000 h at 873 K, $v_{Na} = 1.5\ m\,s^{-1}$) with maximum duration exposed in sodium is Cr = 6.75%, Ni = 3.23% and Fe $\simeq$ 90%.

Leaching rates based on depleted layer widths in SS 316, alloy D9 and SS 304 are presented in Table 5. Leaching rates of AISI type SS 316 are available in Refs. [3,12,13]. Depleted layer widths of alloy D9 exposed to sodium at 773 K are available in Ref. [15]. Leaching rates and depleted layer widths of SS 304 are from present results. From Table 5, we can understand that the leaching rates are comparable for all steels, but alloys without molybdenum, namely, SS 304 develop porosities due to sodium exposure. The actual depleted layer widths obtained using experiments for all steels at higher duration and higher temperature are much higher than the calculated values using the Thorley and Tyzack model. Hence, for life prediction due to sodium corrosion effect, a new model has to be evolved based on the experimental results available. Scanning electron micrographs of sodium exposed SS 304 in cross-section view showing ferrite layer and microcavities due to prolonged exposure are presented in Fig. 4(a) and (b); the formation of carbides due to sodium exposure is shown in Fig. 5. In this figure, we can also observe decohesion of ferrite layer from the matrix.

Compatibility of structural materials with sodium, as experience gained in 40 years of operation of the BR-5/BR-10 reactors, has been reported by Karpov et al. [16]. The steels used in these reactor systems namely Kh18N10T and Kh18N9, after 40 years of exposure to flowing sodium are reported to show good compatibility and no serious corrosion problems except carburization to a large extent. These stainless steels do not contain molybdenum. This observation of steels without molybdenum having very good compatibility in dynamic sodium system is contradicting to our observations. According to Shiels et al. [12], alloys without molybdenum leach at a faster rate as corrosion resistant nodes

Table 3
Comparison of experimental and calculated layer widths for SS 304 specimens

Sodium exposure	Calculated[a] (μm)	Experimental (μm)
80 000 h at 823 K	3.3	12–15
80 000 h at 823 K + 20 000 h at 873 K	4.8	18–20
10 000 h at 973 K	2.2	10–12

[a] Calculated for maximum oxygen content of 2 ppm.

Table 4
Rate of metal loss in sodium, calculated using the Thorley and Tyzack model [8] with sodium velocity of 4–6 m/s

T (K)	Metal loss	Oxygen (ppm)				
		1	2	3	5	10
773	μm/1000 h	0.693×10^{-2}	1.992×10^{-2}	3.660×10^{-2}	7.870×10^{-2}	2.230×10^{-1}
	g/(m^2 h)	0.054×10^{-3}	0.156×10^{-3}	0.286×10^{-3}	0.616×10^{-3}	1.743×10^{-3}
873	μm/1000 h	2.640×10^{-2}	7.555×10^{-2}	1.388×10^{-1}	2.986×10^{-1}	8.446×10^{-1}
	g/(m^2 h)	0.206×10^{-3}	0.591×10^{-3}	1.086×10^{-3}	2.340×10^{-3}	6.610×10^{-3}
973	μm/1000 h	7.610×10^{-2}	2.218×10^{-1}	4.001×10^{-1}	8.610×10^{-1}	2.435
	g/(m^2 h)	0.595×10^{-3}	1.710×10^{-3}	3.130×10^{-3}	6.739×10^{-3}	1.906×10^{-2}

Table 5
Leaching rates based on depleted layer width in SS 316 [3,12,13], D9 [15] and SS 304 (present work)

Treatment	Depletion layer (μm)	Leaching rate (m^2/s)	Remarks
823 K, 80 000 h	12–15	$(1.25–1.95) \times 10^{-19}$	CREVONA-SS 304
823 K, 80 000 h + 873 K, 20 000 h	18–20	$(2.25–2.78) \times 10^{-19}$	CREVONA-SS 304
973 K, 10 000 h	10–12	$(6.94–10) \times 10^{-19}$	CREVONA-SS 304
1028 K, 2500 h	18–20	$(9–11) \times 10^{-18}$	Olander-SS 316 [3]
973 K, 8000 h	27[a]	6×10^{-18}	Shiels-SS 316 [12]
773 K, 3000 h	1.5–2.5	$(1.25–2) \times 10^{-19}$	Alloy D9 [15]
773 K, 500 h	6	5×10^{-17}	SS 316 [13] (annealed, high value)
773 K, 2000 h	8	2.2×10^{-18}	
873 K, 500 h	7	6.8×10^{-18}	
873 K, 2000 h	15	7.8×10^{-18}	

[a] High value compared to others in literature.

are not formed and develop porosities since molybdenum plays an important role in forming corrosion resistant nodes. However, the Russian steels were carburized, and the deposition of carbides $Cr_{23}C_6$ may have suppressed the leaching of chromium from grain boundaries. Thus, grain boundary cavity formation was reduced.

In another observation by Fukutomi et al. [17], molybdenum coating of vanadium by chemical vapour deposition was used to improve and to protect pure vanadium and vanadium alloys from sodium corrosion. In order to eliminate the influence of constituents of the structural material on the corrosion rate, Kolster and Bos [18] have studied the sodium corrosion in molybdenum loop systems. All these observations reinforce the fact that the best corrosion resistant alloys in sodium are those with high molybdenum content or pure molybdenum itself. However, AISI type 304 SS can be considered as a useful container material for sodium.

5. Conclusions

The results of the analytical and metallographic examinations of the sodium exposed material allow to draw some conclusions:

1. Alloys without molybdenum (e.g. AISI 304 SS) can develop porosities in the depleted layers due to high temperature and longer durations of exposure in sodium.
2. The Thorley and Tyzack model is good for comparing laboratory scale experimental results and is not appropriate for long-term exposure and life prediction of components made of stainless steel AISI 304 exposed to sodium.
3. The corrosion of stainless steel AISI 304 was found to be such that the material can be considered as a useful container material for sodium cooling systems, though austenitic steels containing molybdenum are better compatible with the liquid metal.

Acknowledgements

The authors wish to thank Dr G. Periaswami, Head, Materials Chemistry Division and Dr Baldev Raj, Director, Materials, Chemistry and Reprocessing Group, IGCAR for constant encouragement and support.

References

[1] I.R. Cameron, Nuclear Fission Reactors, Plenum, New York, 1982, p. 282.
[2] H.U. Borgstedt, C.K. Mathews, Applied Chemistry of Alkali Metals, Plenum, New York, 1987.
[3] D.R. Olander, Fundamental aspects of nuclear reactor fuel elements, USAEC Report TID-26711-P1, 1976, p. 361.
[4] T. Suzuki, I. Mutoh, T. Yagi, Y. Ikenaga, J. Nucl. Mater. 139 (1986) 97.
[5] T. Suzuki, I. Mutoh, J. Nucl. Mater. 140 (1986) 56.
[6] T. Suzuki, I. Mutoh, J. Nucl. Mater. 152 (1988) 343.
[7] H.U. Borgstedt, in: J.M. Dahlke (Ed.), Proc. Second Int. Conf. on Liquid Metal Technology in Energy Production, CONF-800401-P1, Richland, Washington, 1980, p. 7-1.
[8] A.W. Thorley, C. Tyzack, Liquid Alkali Metals, BNES, London, 1973, p. 257.
[9] H.U. Borgstedt, H. Huthmann, J. Nucl. Mater. 183 (1991) 127.
[10] A.R. Keeton, C. Bagnall, in: J.M. Dahlke (Ed.), Proc. Second Int. Conf. on Liquid Metal Technology in Energy Production, CONF-800401-P1, Richland, Washington, 1980, p. 7-18.
[11] Kolster, in: J.M. Dahlke (Ed.), Proc. Second Int. Conf. on Liquid Metal Technology in Energy Production, CONF-800401-P1, Richland, Washington, 1980, p. 7-53.
[12] C.B. Shiels, A.R. Keeton, R.E. Witkowski, R.P. Anantamula, in: J.M. Dahlke (Ed.), Proc. Second Int. Conf. on Liquid Metal Technology in Energy Production, CONF-800401-P1, Richland, Washington, 1980, p. 7-11.

[13] Vaidehi Ganesan, V. Ganesan, J. Nucl. Mater. 256 (1998) 69.
[14] H.U. Borgstedt, G. Drechsler, G. Frees, E. Wollensack, in: H.U. Borgstedt (Ed.), Material Behaviour and Physical Chemistry in Liquid Metal Systems, Plenum, New York, 1982, p. 185.
[15] Vaidehi Ganesan, PhD thesis, 1999, University of Madras, India.
[16] A.V. Karpov, M.Kh. Kononyuk, L.I. Mamaev, Yu.L. Kulikov, At. Energy 91 (2001) 951.
[17] M. Fukutomi, M. Okada, R. Watnabe, J. Less-Common Met. 48 (1976) 65.
[18] B.H. Kolster, L. Bos, in: Proc. Third International Conference on Liquid Metal Engineering and Technology, Oxford, 1984, vol. 1, The British Nuclear Energy Society, London, 1984, p. 9.